# Influence of Hydrogen Bonding in the Paramagnetic NMR Shieldings of Nitronylnitroxide Derivative Molecules

**Lyudmyla Telyatnyk,*,† Juha Vaara,‡ Zilvinas Rinkevicius,† and Olav Vahtras†**

*Laboratory of Theoretical Chemistry, Department of Biotechnology, SCFAB, The Royal Institute of Technology, SE-10691, Sweden, and Department of Chemistry, P.O. Box 55 (A.I. Virtasen aukio 1), FIN-00014 University of Helsinki, Finland*

*Received: May 30, 2003; In Final Form: November 10, 2003*

We apply our recently developed methodology for first-principles computations of paramagnetic NMR shieldings and explore the shieldings in a selected set of radicals that form core units in molecular magnets. The influence on these parameters of hydrogen bonding, that corresponds to the crystal environment, is the prime objective of the study. Nitronylnitroxide radicals with the hydroxyphenyl group in the ortho, meta, and para positions, as well as *p*-methoxyphenyl derivatives, are chosen for this purpose. The strong NO···HO hydrogen bonding in the real crystal structure has been simulated by adding water molecules in the twelve molecular complexes investigated. Comparison of calculated and experimental data is made by taking the special features of the solid state and solution environments into account. The observed change in the shielding constant due to hydrogen bonding is explained by the spin delocalization picture; the dominating contribution is the temperature-dependent contact shielding containing the isotropic hyperfine coupling constant.

## Introduction

Among the exceedingly abundant organic chemical compounds in nature, only a few are magnetically active due to the presence of unpaired electrons.[1] A family of unusually electro- and thermochemically stable nitronylnitroxide (NN) radicals takes a very special place among these few and were synthesized first by Osiecki and Ullman more than 30 years ago.[2] Historically, the primary use of nitroxide derivatives has concerned spin labeling for structural analysis, including paramagnetic marking for EPR spectroscopy, as well as spin trapping for biological studies of functional and bonding features of cell membranes and other structures of interest in the life sciences.[3−5] The interest in these compounds increased in 1973, owing to the discovery of weak ferromagnetic ordering in the biradical suberate of the TANOL molecule[6] and later to the discovery of the first really pure organic magnet, namely, *p*-nitrophenyl nitronylnitroxide, as late as 1991.[7,8] Now the number of such compounds is increasing rapidly[9] despite some troublesome disadvantages such as low magnetic ordering temperatures as well as rigid requirements for the crystal organization.[10,11]

Although several types of organic magnetic compounds are known by now,[12−14] the NN radicals hold a special position. They form crystals containing only one type of elementary molecules that alternate in a well-defined order and, in the simplest cases, do not contain any impurities.[10] The magnetic properties of nitroxide crystals are therefore determined mostly by the electronic structure of the molecule itself. The spatial orientation and conformations of the individual molecules become crucial aspects, too. It is important to be able to change the conformation of single molecular units in order to maximize the number of intermolecular contacts and, at the same time, to minimize the energy of the connected complex.[15] Other physical effects originating in the intermolecular interactions, such as electrostatic interactions, charge transfer, and hydrogen bonding,[15] also play significant roles in the magnetic ordering. NNs tend to form hydrogen-bonding networks that allow the propagation of magnetic interactions and spin polarization in the crystal.[16]

The spin distribution of NNs can be investigated in detail by the electron paramagnetic resonance (EPR) and NMR spectroscopic methods[17,18,19,20,21,22] and by theoretical calculations.[23,24] The crucial characteristics of NNs, as paramagnetic systems, derive from the large spectral widths and short relaxation times that call for special techniques of spectral registration.[25,26] Solid-state magic-angle spinning (MAS) NMR is one of the methods for investigating NN radicals.[27]

MAS NMR investigations of NN-derivative compounds[28,29] have provided relevant data such as the spatial distribution of the sign and the magnitude of the spin density, which are important features from the point of view of magnetic molecular interaction.[30,11,31] The electron spin density on the nucleus can be directly evaluated from the hyperfine shift $\delta^{con}$. Therefore, a determination of $\delta^{con}$ from the experimental NMR spectra of paramagnetic molecules is a principal step. Between the two possibilities to determine $\delta^{con}$, by performing the temperature-dependent measurements or by subtracting the chemical shift $\delta^0$ of a similar diamagnetic compound from the observed chemical shift $\delta^{exp}$ of the paramagnetic species, the second one is usually preferred by experimentalists. However, the neglect of the change of the orbital contribution to the shielding in paramagnetic systems in comparison to the diamagnetic one may be a questionable procedure. In fact, it may account for most of the deviations between calculated and experimentally determined $\delta^{con}$ values.

The diamagnetic and second-order paramagnetic contributions present in the nuclear shielding of paramagnetic molecules are analogous to the conventional expressions of Ramsey[32] for

* Author to whom correspondence may be addressed. E-mail: luda@theochem.kth.se.

† The Royal Institute of Technology.

‡ University of Helsinki.

10.1021/jp030693g CCC: $27.50 
Published on Web 12/20/2003

closed-shell molecules, and the sum of these contributions forms the orbital part of the nuclear shielding of paramagnetic molecules. The total shielding tensor in a paramagnetic molecule contains, in turn, temperature-dependent isotropic contact as well as temperature-dependent anisotropic dipolar and orbital-shielding parts.[33]

Theoretical calculations of NMR parameters are of great importance, as the assignment and interpretation of experimental spectra is not straightforward, and present a wide field for the development of new theoretical models. In the present paper, we use our recently developed method dealing with the case of small spin−orbit coupling consistent up to $O(\alpha^2)$, where $\alpha$ is the fine-structure constant, for the calculation of isotropic shielding constants for derivatives of phenyl nitronylnitroxide radicals. The strong hydrogen bonds of the type NO···HO, that characterize the real crystal structures of these compounds, are simulated by adding water molecules. For all molecular complexes, we calculate the contact and orbital contributions to the shielding constants that subsequently are converted into chemical-shift values and compared with experimental data. The main point of our investigation is to explore the tendency of delocalization of the unpaired electron through the change of the NMR signal shifts along with the change of the amount of hydrogen bonds per molecule.

### Nuclear Shielding in Paramagnetic Molecules

According to our previous work,[33] the nuclear-shielding tensor of a paramagnetic molecule may in the case of small spin−orbit coupling be written for nucleus $K$ as

$$\boldsymbol{\sigma}_K = \boldsymbol{\sigma}_K^{\mathrm{con}} + \boldsymbol{\sigma}_K^{\mathrm{dip}} + \boldsymbol{\sigma}_K^{\mathrm{orb}} \tag{1}$$

where $\boldsymbol{\sigma}_K^{\mathrm{con}}$ and $\boldsymbol{\sigma}_K^{\mathrm{dip}}$ are the temperature-dependent contact and dipolar terms arising from the corresponding, averaged, hyperfine interaction in an ensemble of electronic spin Zeeman levels. The $\boldsymbol{\sigma}_K^{\mathrm{con}}$ and $\boldsymbol{\sigma}_K^{\mathrm{dip}}$ are unique features of paramagnetic molecules. The Cartesian tensor components of these terms can be expressed via the hyperfine coupling tensor, $\boldsymbol{A}_K$, as

$$\sigma_{K,\epsilon\tau}^{\mathrm{con}} = -\frac{\pi}{\gamma_K} A_{K,\mathrm{iso}} \delta_{\epsilon\tau} g_{\mathrm{e}} \frac{S(S+1)}{3kT} \tag{2}$$

$$\sigma_{K,\epsilon\tau}^{\mathrm{dip}} = -\frac{\pi}{\gamma_K} A_{K,\epsilon\tau}^{\mathrm{dip}} g_{\mathrm{e}} \frac{S(S+1)}{3kT} \tag{3}$$

where $A_{\mathrm{iso}}$ is the isotropic hyperfine coupling constant, $A_{\epsilon\tau}^{\mathrm{dip}}$ is the dipolar hyperfine coupling tensor element, and $S$ is the spin of the paramagnetic molecule. $\sigma_{\mathrm{K},\epsilon\tau}^{\mathrm{dip}}$ is symmetric in the two indices $\epsilon\tau$ and does not contribute to the isotropic nuclear-shielding constant, $\sigma_K = {}^1/_3 Tr\boldsymbol{\sigma}_K$, for rapidly tumbling molecules, but it affects the shielding anisotropy. The last term in eq 1, $\boldsymbol{\sigma}_K^{\mathrm{orb}}$, is analogous to the orbital shielding in closed-shell molecules and comprises both dia- and paramagnetic parts, $\boldsymbol{\sigma}_K^{\mathrm{dia}}$ and $\boldsymbol{\sigma}_K^{\mathrm{para}}$, respectively.[33] The $\boldsymbol{\sigma}_K^{\mathrm{orb}}$ contributes both to $\sigma_K$ and to the anisotropy of the shielding.

From the experimentalists' point of view, the most important quantity in a MAS NMR experiment for paramagnetic molecules is the chemical shift of the resonating nucleus, which usually is defined with respect to a suitable reference system

$$\delta^{\mathrm{exp}} = \delta^0 + \delta^{\mathrm{con}} + \delta^{\mathrm{pc}} \tag{4}$$

where $\delta^0$ is taken to be the chemical shift of a "similar" diamagnetic compound, $\delta^{\mathrm{con}}$ represents the contact shift arising from $\boldsymbol{\sigma}_K^{\mathrm{con}}$, and $\delta^{\mathrm{pc}}$ is the pseudocontact shift.[25] $\delta^{\mathrm{pc}}$ has been neglected in our theoretical investigation as it becomes important only in the case of large spin−orbit coupling. As shown in our previous paper,[33] the use of the chemical shifts of analogous diamagnetic compounds, $\delta^0$, neglects the changes of $\boldsymbol{\sigma}_K^{\mathrm{orb}}$ when going from the diamagnetic to the paramagnetic molecule. Hence, eq 4 is a potential source of large errors for determining the contact shift $\delta^{\mathrm{con}}$ from the observed $\delta^{\mathrm{exp}}$. Therefore, we calculate $\sigma_K^{\mathrm{orb}}$ explicitly and define the chemical shift as

$$\delta = \sigma_{\mathrm{iso}}^{\mathrm{ref}} - \sigma_{\mathrm{iso}} = \sigma_{\mathrm{iso}}^{\mathrm{ref}} - \sigma_{\mathrm{iso}}^{\mathrm{orb}} - \sigma_{\mathrm{iso}}^{\mathrm{con}} = \delta^{\mathrm{orb}} + \delta^{\mathrm{con}} \tag{5}$$

Here, $\sigma_{\mathrm{iso}}^{\mathrm{orb}} = {}^1/_3 Tr\boldsymbol{\sigma}^{\mathrm{orb}}$ is the isotropic orbital nuclear shielding and $\sigma_{\mathrm{iso}}^{\mathrm{ref}}$ is the shielding constant of the resonating nucleus of the diamagnetic reference compound. Similarly, the contact shift in our theoretical calculations is defined as

$$\delta^{\mathrm{con}} = -\sigma_{\mathrm{iso}}^{\mathrm{con}} \tag{6}$$

lacking, of course, the corresponding contribution in a closed-shell reference system.

### Computational Details

**Structural Models.** The group of the simple hydroxy- (See Figure 1) and methoxy-substituted (see the first molecule in Figure 2) phenyl nitronylnitroxide molecules have been chosen as a starting point in our investigation. For the modeling of a possible hydrogen bond formation, we used the two NO groups of the imidazolyl ring, active for hydrogen bonding, and one OH group at three different positions in the phenyl ring, ortho (denoted 2-OH in Figure 1), meta (3-OH), and para (4-OH). The simplest approach to model the influence of hydrogen bonding is to add a certain number of water molecules at the sites of neighboring molecules in the crystal. By considering systems having 1−3 (for hydroxy-substituted compounds) or 1−2 (for methoxy-substituted ones) hydrogen bonds per molecule, we obtained a set of twelve isolated molecules and molecular complexes to be calculated (Figures 1−4).

The geometries of all the compounds were optimized using the restricted open-shell (RO) density functional theory (DFT) method in the Gaussian 98 code[34] with the hybrid B3LYP functional[35] and 6-31G(d,p) basis set. The main body of known geometry optimizations of medium-size open-shell systems use unrestricted methods,[23,36] and we have therefore made additional geometry optimization of the *o*-hydroxyphenyl nitronylnitroxide (2-OHPhNN) at the UB3LYP level with the same basis set for the purpose of validating the results. The similar magnitude of the nitrogen−oxygen and nitrogen−carbon bond distances, as well as the angles in the imidazolyl ring, justifies the RO procedure.

**Calculations of Chemical Shifts.** The unrestricted DFT calculations of $\sigma_{\mathrm{iso}}$ have been divided into two parts. Optimized structures of the NNs have been used in the calculation of the orbital contribution to the open-shell shielding tensors using the deMon software.[33,37,38,39] In choosing the computational parameters, we took into account the results of the extensive investigation in our previous work.[33] Accordingly, the contracted IGLO-III basis set[40,41] and Perdew-86 (P86)[42,43] generalized gradient approximation (GGA) exchange-correlation functional were chosen as the most suitable. The FINE angular grid with 32 radial points (F32)[37] was applied.

Auxiliary basis sets of Gaussian functions, denoted (5,1;5,1) for H and (5,2;5,2) for first-row atoms were used for the fitting

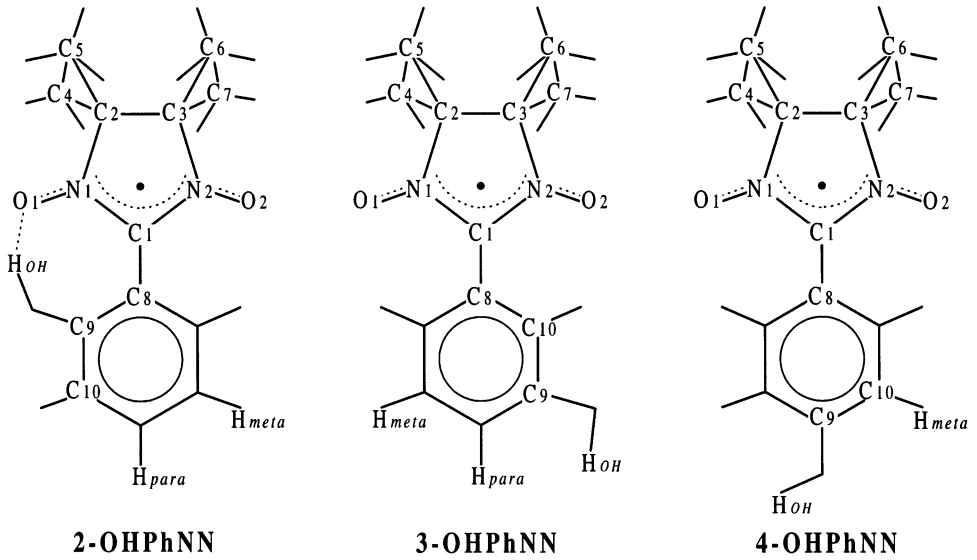


**Figure 1.** Numbering system of the atoms for selected nitronylnitroxides with emphasis on the *o*-, *m*-, and *p*-hydroxyphenyl derivatives.

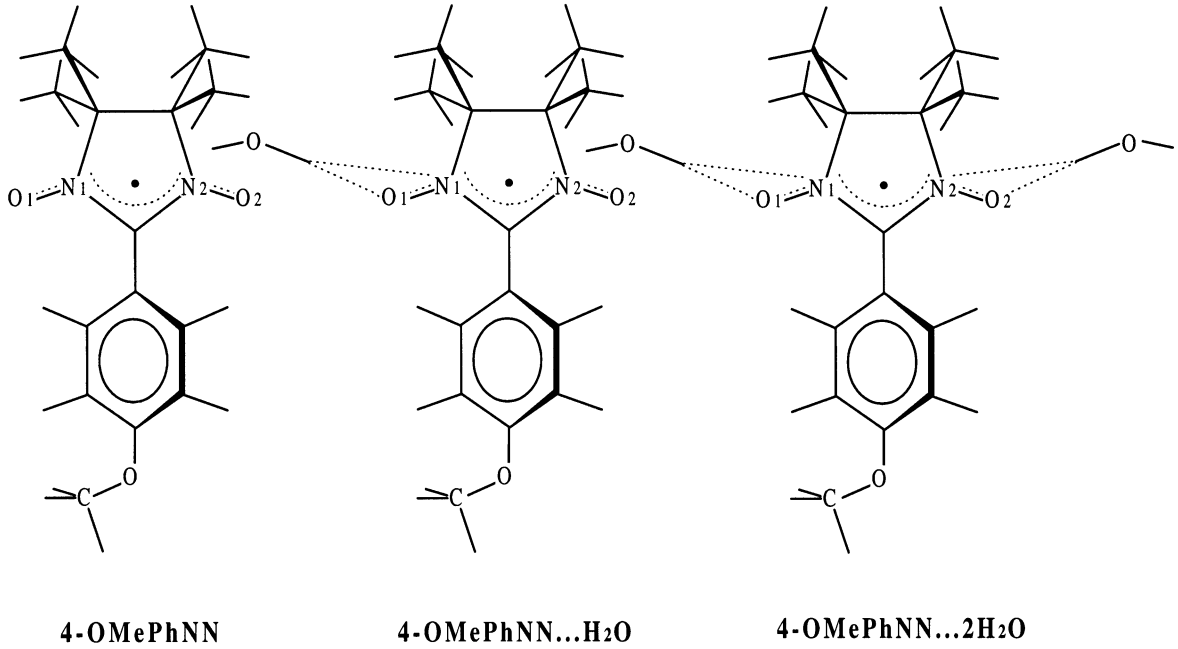


**Figure 2.** Methoxyphenyl nitronylnitroxide and its complexes with *n* water molecules ($n = 1, 2$).

of the charge density (defined by the first two numbers corresponding to the number of s primitives and spd shells, respectively, in the above notation) and exchange-correlation potentials (the last two numbers). The orbital contributions to $\sigma_{iso}$ were calculated with the individual gauges for localized orbitals (IGLO)[41] method, using localization of all occupied MOs in one group in accordance with the Pipek−Mezey[44] method (IGLO PM).[45] The uncoupled sum-over-states (SOS)[46] method was used, as appropriate for nonhybrid DFT with the current density dependence[47] of the exchange-correlation functional neglected.

The $\sigma^{con}$ part was calculated with UDFT using the B3LYP functional in the Gaussian 98 program in order to obtain improved descriptions of the spin density in comparison with GGA.[33] Values were evaluated at 314 K for $^{13}C$ and at 305 and 314 K for $^{1}H$.

To compare with the experimental $^{1}H$ and $^{13}C$ data of ref 29, the calculated shielding constants were converted to chemical shifts with respect to the diamagnetic adamantane molecule. $\sigma_{iso}^{ref}$ of adamantane was obtained in the same manner as in ref 33.

## Results and Discussion

**Geometry.** The results of the geometry optimization are presented in Table 1. We are using here the usual chemical notation for each molecule, in common *n*-OH(OMe)PhNN. Only the most important bond distances and angles that concern the nitroxide ring and hydrogen bonds are reported. For convenience, the known experimental results are divided into two groups denoted *experimental* for the ortho-substituted molecules, for which much experimental data exist, and *mean experimental* for the remaining molecules, where such data is more scarce.

All computed data are close to the experimental values, with a few exceptions. First of all, the evident imbalance between the calculated NO bond distances, that does not observe experimentally,[48] occurs especially for the ortho-substituted compound. Contrary to the other *n*-OH(OMe)PhNN systems, 2-OHPhNN is characterized by an intramolecular hydrogen bond

**TABLE 1: Geometry Optimization Results for a Set of Nitronylnitroxide Derivative Molecules[a]**

| type of compound | $r(N_1O_1)$ | $r(N_2O_2)$ | $r(N_1C_1)$ | $r(N_2C_1)$ | $r(OH\cdots O)$ | $\angle N_1C_1N_2$ | $\angle_{av}C_1N_2C_3$ | $\angle C_1N_2C_3C_2$ |
|---|---|---|---|---|---|---|---|---|
| Ortho-Substituted Compound | | | | | | | | |
| 2-OHPhNN[b] | 1.270 | 1.295 | 1.376 | 1.345 | 1.580 | 107.95 | 112.36 | −20.94 |
| 2-OHPhNN[c] | 1.270 | 1.290 | 1.380 | 1.330 | 1.565 | 108.05 | 112.33 | −21.02 |
| exp[d] | 1.274−1.283 | 1.277−1.300 | 1.325−1.347 | 1.317−1.339 | 1.519−1.569 | 109.10 | 112.20−117.9 | −21.00 |
| Meta-Substituted Complexes | | | | | | | | |
| 3-OHPhNN | 1.276 | 1.275 | 1.361 | 1.361 | | 108.37 | 111.96 | −20.62 |
| 3-OHPhNN·$H_2O$ | 1.276 | 1.276 | 1.360 | 1.361 | 1.840 | 108.39 | 111.99 | −20.48 |
| 3-OHPhNN·$2H_2O$ | 1.278 | 1.276 | 1.359 | 1.356 | 1.792 | 108.91 | 111.83 | −20.22 |
| 3-OHPhNN·$3H_2O$ | 1.279 | 1.276 | 1.349 | 1.364 | 1.786 | 108.89 | 111.91 | −20.00 |
| Para-Substituted Complexes | | | | | | | | |
| 4-OHPhNN | 1.279 | 1.278 | 1.360 | 1.362 | | 108.22 | 112.07 | −20.68 |
| 4-OHPhNN·$H_2O$ | 1.279 | 1.278 | 1.361 | 1.362 | 1.811 | 108.12 | 112.11 | −20.74 |
| 4-OHPhNN·$2H_2O$ | 1.289 | 1.276 | 1.349 | 1.371 | 1.800 | 108.05 | 112.08 | −21.84 |
| 4-OHPhNN·$3H_2O$ | 1.285 | 1.284 | 1.358 | 1.358 | 1.800 | 108.06 | 112.14 | −22.40 |
| Methoxy-Substituted Complexes | | | | | | | | |
| 4-OMePhNN | 1.279 | 1.278 | 1.360 | 1.362 | | 108.20 | 112.07 | −20.71 |
| 4-OMePhNN·$H_2O$ | 1.275 | 1.287 | 1.368 | 1.350 | | 108.27 | 112.04 | −21.45 |
| 4-OMePhNN·$2H_2O$ | 1.284 | 1.283 | 1.356 | 1.358 | | 108.21 | 112.05 | −22.40 |
| mean exp[e] | 1.270−1.285 | 1.272−1.283 | 1.345−1.355 | 1.341−1.364 | 1.653−1.870 | 109.00−109.30 | 112.25 | −21.00 |

[a] See Figure 1 for the numbering (the numbering of 4-OMePhNN is analogous to 4-OHPhNN). Bond distances are in angstroms, and angles are in degrees. [b] Initial guess UHF, after that UB3LYP optimization. Basis 6-31G(d,p). $\angle OH\cdots O = 162.90°$. [c] Here and in the following: initial guess ROHF, after that ROB3LYP optimization. Basis 6-31G(d,p). $\angle OH\cdots O = 162.86°$ (experiment: 163.00−163.50° [49,13]). [d] Experimental data from refs 26, 49, 13, and 50. [e] Experimental data from refs 26, 48, 36, and 52.

that is formed between one of the nearest NO groups in the imidazolyl ring and the ortho OH group in the same molecule.[13] The remaining molecules have a tendency of forming intermolecular hydrogen bonds. By this fact, one can also explain the difference between NC bond distances[36] of the imidazolyl ring that in our calculation are slightly underestimated.

The calculated hydrogen-bond distances must as well as possible correspond to those in the experimental crystal structure.[13] The hydrogen bonds fall into two categories. Strong bonds are mainly localized in the H-bond active sites of the molecules, such as the OH and NO groups in *n*-OH(OMe)PhNN. The weak hydrogen bonds are localized mainly in the $CH_3$ groups. We have only considered the strong type, and the $r(OH\cdots O)$ data in Table 1 are defined for the bond between the hydrogen in the OH group of the phenyl ring and the available hydrogen bond donor like oxygen of water in our theoretical model. We stress here the good correspondence between the experimental[13,49] and calculated data.

Other principal characteristics of the *n*-OH(OMe)PhNN group of molecules are the two angles, the deformation angle of the imidazolyl ring denoted $\angle C_1N_2C_3C_2$ in Table 1 and the twist angle[50] between the hydroxyphenyl and NCN elements of the imidazolyl ring (not presented in Table 1). Investigations of the crystal structure indicate that combinations of these two angles into enantiomeric or pseudoeclipsed conformations are preferred[51] for all members of the *n*-OH(OMe)PhNNs group of molecules. Our optimized structures have an organization of angles that exactly corresponds to the crystallographic data.

A special feature for all PhNN molecules is the −21.0° deformation angle,[26] $\angle C_1N_2C_3C_2$, in the imidazolyl ring. This parameter is mainly constant also during the process of crystal formation and must be reproduced in any meaningful theoretical geometry optimization. Our results are well arranged around this value.

The NCN angle (denoted $\angle N_1C_1N_2$ in Table 1) and the average CNC angle ($\angle_{av}C_1N_2C_3$) of the imidazolyl ring are presented in order to assess the quality of the geometry optimization. The agreement with the experimental[36] and other calculated data[52] is, in general, good for the second angle but poor for the first one.

**$^{13}$C NMR Data.** The calculated values for the $^{13}$C NMR chemical shifts are presented in Table 2 along with the corresponding experimental MAS NMR data from ref 29. As mentioned above, the fact that the organization of the crystal structure for each type of molecule can be defined as weakly or strongly bonding is also important for the analysis of the chemical-shift data. While the 2-OHPhNN molecule is characterized by the strong intramolecular hydrogen bond that connects the ortho hydroxy and the nearest iminoxyl group (See Figure 1), the formation of two strong intermolecular hydrogen bonds is favored by the meta-substituted molecules. Each hydroxy group of the phenyl ring couples with the ON group of the imidazolyl ring of the adjacent molecule. The coupling occurs in a head-to-tail manner and results in dimerization.[13,53] Two strong hydrogen bonds determine the unit formation of the para-substituted molecules. The OH group at the fourth position of the phenyl ring in one molecule is bonded with the ON group of the next molecule. The molecules form a chain structure,[20,13,24,50] where the identical structural elements are connected by two hydrogen bonds. The weak CH···ON bond between the methyl and iminoxide groups of imidazolyl ring defines the connection of molecular chains to each other in all of these crystals.

Yet another situation is prevalent for the methoxy-substituted group of molecules, as only weak bonds are formed.[54] There are no hydroxy groups in the phenyl ring and crystal bonding occurs mainly by bimolecular interactions between the ON groups and the hydrogen atoms of the phenyl ring.[55,56] The resulting structure is similar to the meta-substituted case results.

Among different effects that are important for the outcome of MAS NMR experiments, the contribution from hydrogen bonding[27] is crucial. A correspondence between the experimental crystal structure and the molecular model is therefore required. We expect that the 2-OHPhNN (the RODFT structure), 3-OHPhNN·$2H_2O$, 4-OHPhNN·$2H_2O$, and 4-OMePhNN·$H_2O$ systems allow a comparison of their computed chemical shifts with the experimental ones obtained in the solid state.

The trend of the magnitude and sign is rather similar between the experimental[29] and calculated data, with no systematic tendency of either over- or underestimation. For the 2-OHPhNN

**TABLE 2: $^{13}$C NMR Chemical Shifts ($\delta$, in ppm) for *n*-OH(OMe)PhNNs and Their Complexes with *n* Water Molecules ( $n$ = 1, 2, 3)[a]**

| type of compound | $C_1$ | $C_2$ | $C_3$ | $C_4$ | $C_5$ | $C_6$ | $C_7$ | $C_8$ | $C_9$ | $C_{10}$ |
|---|---|---|---|---|---|---|---|---|---|---|
| Ortho-Substituted Compound | | | | | | | | | | |
| 2-OHPhNN | −3388 | −413 | −711 | 939 | 370 | 414 | 1196 | 846 | −349 | 247 |
| 2-OHPhNN | −3264 | −370 | −741 | 863 | 342 | 444 | 1269 | 794 | −318 | 224 |
| exp[b] | | −309 | −750 | 705 | 360 | 402 | 1180 | | −225 | 238 |
| Meta-Substituted Complexes | | | | | | | | | | |
| 3-OHPhNN | −3554 | −590 | −619 | 979 | 357 | 368 | 989 | 821 | 327 | −150 |
| 3-OHPhNN·$H_2O$ | −3371 | −603 | −588 | 976 | 366 | 366 | 975 | 761 | 276 | −90 |
| 3-OHPhNN·$2H_2O$ | −3659 | −632 | −635 | 1020 | 399 | 378 | 1006 | 869 | 321 | −200 |
| 3-OHPhNN·$3H_2O$ | −3583 | −571 | −676 | 957 | 364 | 399 | 1119 | 865 | 333 | −297 |
| exp | | −617 | −707 | 1030 | 568 | 568 | 1075 | 700 | 320 | −118 |
| Para-Substituted Complexes | | | | | | | | | | |
| 4-OHPhNN | −3471 | −600 | −613 | 971 | 385 | 389 | 985 | 754 | −22 | 231 |
| 4-OHPhNN·$H_2O$ | −3389 | −603 | −595 | 981 | 389 | 386 | 988 | 857 | −119 | 361 |
| 4-OHPhNN·$2H_2O$ | −3584 | −615 | −610 | 1105 | 310 | 343 | 1166 | 843 | −43 | 280 |
| 4-OHPhNN·$3H_2O$ | −3391 | −595 | −611 | 1251 | 272 | 275 | 1256 | 736 | 26 | 216 |
| exp | | −367 | −633 | 1080 | 309 | 363 | 1250 | 704 | 25 | 241 |
| Methoxy-Substituted Complexes | | | | | | | | | | |
| 4-OMePhNN | −3501 | −604 | −612 | 975 | 385 | 388 | 989 | 822 | −84 | 308 |
| 4-OMePhNN·$H_2O$ | −3504 | −609 | −611 | 1148 | 345 | 317 | 1113 | 822 | −39 | 276 |
| 4-OMePhNN·$2H_2O$ | −3441 | −595 | −601 | 1237 | 271 | 273 | 1255 | 764 | 33 | 210 |
| exp | | −470 | −590 | 1060 | 332 | 418 | 1145 | 727 | −4 | 268 |

[a] Results were derived using the formula $\delta = \sigma_{iso}^{ref} - \sigma_{iso}^{orb} - \sigma^{con} + \delta^0$. The $^{13}CH_2$ signal, experimentally at $\delta^0 = 29.5$ ppm, in adamantane was used as an external chemical shift reference. UKS/IGLO-III/F32 calculation with the P86 exchange-correlation functional gives $\sigma_{iso}^{ref}$ ($^{13}$C) = 132.3 ppm for the reference system from ref 33. [b] Experimental MAS NMR data from ref 29.

(the RODFT structure), 3-OHPhNN·$2H_2O$, 4-OHPhNN·$2H_2O$, and 4-OMePhNN·$H_2O$ systems, the calculated and experimental data are found to correlate to a large degree. The main sources of error are limitations in the DFT methodology, basis set errors, as well as matrix effects (beyond that described by the present strong hydrogen bonds), and motional averaging.

In general, there is a good correlation between the calculated and experimental data, but several exceptions can be distinguished. There is a considerable underestimation, by a factor of 1.5, of the $C_5$ and $C_6$ chemical shifts of 3-OHPhNN·$2H_2O$ as well as an overestimation, by a factor of 1.7, of the $C_2$ chemical shift of 4-OHPhNN·$2H_2O$. First, these observations can be explained by features of the chosen molecular models. The addition of water molecules produces very strongly bonded complexes since the donor−acceptor ability of $H_2O$ is large. In the real crystal, the bonding must be weaker.[56] On the other hand, we do not include the weak CH···ON interaction that may have an effect on the chemical shifts of the methyl carbons. Second, the lack of convergence with experimental data in these cases can be caused by DFT errors in the calculated spin densities due to poor treatment of the spin-polarization contributions from the doubly occupied orbitals when the direct SOMO contribution is small.

The experimentally missing $C_1$ chemical shift of the imidazolyl ring is estimated in our investigation to be −3659 ppm at maximum of absolute value, which is comparable to the single experimentally known value for *o*-tolylnitronylnitroxide,[57] −3550 ppm.

The total shielding constants are divided into two parts, orbital and contact, in Table 3. The $\sigma_{iso}^{orb}$ values are positive for all carbons, indicating that the first-order $\langle 0|H_{K,B_0}^{DS}|0\rangle$ contribution to $\sigma^{orb}$ [33] is predominant, i.e., it has a diamagnetic character. Nevertheless, the second-order paramagnetic contribution to $\sigma^{orb}$ is essential too. As expected, in this $\pi$ radical, the unpaired electron is delocalized between nitrogens and oxygens in imidazolyl ring and simultaneously influences the carbons, with the main weight in $C_1$.[56] That atom has, accordingly, the smallest relative orbital contribution among all the carbons in the imidazolyl ring, about 30.2 ppm in 3-OHPhNN·$2H_2O$, which we consider in this section as an example. The first-order contribution to $\sigma^{orb}$ of $C_1$ in this complex is estimated to be 257.9 ppm and the second-order −227.7 ppm. The orbital part obtained for the $C_2$ (94.5 ppm) and $C_3$(93.7 ppm) nuclei are almost equal; the second-order orbital parts, −153.6 and −154.0 ppm, respectively, are smaller in absolute value than for $C_1$, while the first-order contributions of 248.2 and 247.7 ppm are comparable with those of $C_1$. The orbital shielding values of the methyl carbons are different for axial ($C_4$ and $C_7$ in Figure 1) and equatorial atoms ($C_5$ and $C_6$). This is due to efficient hyperconjugation between the delocalized MO at the nitrogens and the axial bonds and result in the reduction of $\sigma^{orb}$ for $C_4$ (151.4 ppm) and $C_7$ (151.3 ppm) in comparison with $\sigma^{orb}$ of $C_5$ and $C_6$ (156.9 ppm for both nuclei). The first-order orbital contributions are almost equal, 246.9 ppm for axial and 246.5 ppm for equatorial nuclei, while the second-order orbital contributions (−95.7 ppm for $C_4$, −95.6 ppm for $C_7$, and −89.6 ppm for $C_5$ and $C_6$) differ.

$\sigma_{iso}^{orb}$ of $C_9$ has small values in the range of 5.4−10.1 ppm. An analysis of $\sigma^{orb}$ shows that such a small magnitude is mainly caused by the large negative second-order orbital contribution (−244.6 ppm at 3-OHPhNN·$2H_2O$ complex, for example), essentialy due to the influence of the neighboring oxygen. At the same time, the first-order diamagnetic orbital contributions are very similar for all carbons in the phenyl ring, 259.3 ppm for $C_8$, 254.6 ppm for $C_9$, and 259.7 ppm for $C_{10}$.

**$^1$H NMR Data.** The $^1$H chemical shifts, presented in Table 4, were calculated at two temperatures, 305 and 314 K, to compare with experimental solution data, as well as MAS NMR data from ref 29. One can discern several trends in the calculated data. The averaged chemical shifts of the methyl hydrogens, denoted $^1H^{ax/eq}$, correlate well with the experimental ones from NMR in solution. The same holds for the $^1H_{meta}$ shift. The $^1H_{para}$ chemical shifts were experimentally measured at 305 K in solution and at 314 K in the solid state.[29] The agreement between calculated and experimental solid-state shifts for the meta-substituted complex is better than that for the calculated and

**TABLE 3: $^{13}$C Isotropic Shielding Constants (in ppm) for *n*-OH(OMe)PhNNs and Their Complexes with *n* Water Molecules ( *n* = 1, 2, 3)[a,b]**

| nucleus | contributions | no. water molecules | | | | | | | | | | | | |
|---|---|---|---|---|---|---|---|---|---|---|---|---|---|---|
| | | *ortho*- | | *m*-OHPhNNs | | | | *p*-OHPhNNs | | | | *methoxy*-PhNNs | | |
| | | 0[b] | 0[c] | 0 | 1 | 2 | 3 | 0 | 1 | 2 | 3 | 0 | 1 | 2 |
| $C_1$ | $\sigma_{iso}^{orb}$ | 24.3 | 24.6 | 31.3 | 30.9 | 30.2 | 28.8 | 31.8 | 31.7 | 30.6 | 29.7 | 31.7 | 30.7 | 30.0 |
| | $\sigma^{con}$ | 3525 | 3401 | 3684 | 3502 | 3791 | 3716 | 3601 | 3519 | 3716 | 3523 | 3631 | 3635 | 3573 |
| | $\sigma_{iso}$ | 3549 | 3426 | 3715 | 3533 | 3821 | 3745 | 3633 | 3551 | 3747 | 3553 | 3663 | 3666 | 3603 |
| $C_2$ | $\sigma_{iso}^{orb}$ | 95.1 | 94.8 | 94.1 | 94.5 | 94.5 | 93.5 | 94.4 | 94.9 | 93.3 | 92.1 | 94.5 | 93.4 | 91.6 |
| | $\sigma^{con}$ | 480 | 437 | 658 | 670 | 699 | 640 | 667 | 670 | 683 | 665 | 671 | 678 | 666 |
| | $\sigma_{iso}$ | 575 | 532 | 752 | 765 | 794 | 734 | 761 | 765 | 776 | 757 | 766 | 771 | 758 |
| $C_3$ | $\sigma_{iso}^{orb}$ | 92.3 | 92.6 | 94.1 | 94.4 | 93.7 | 93.7 | 94.5 | 95.0 | 93.9 | 92.1 | 94.5 | 92.8 | 91.7 |
| | $\sigma^{con}$ | 780 | 810 | 687 | 655 | 702 | 744 | 680 | 662 | 678 | 681 | 679 | 680 | 671 |
| | $\sigma_{iso}$ | 872 | 903 | 781 | 749 | 796 | 838 | 775 | 757 | 772 | 773 | 774 | 773 | 763 |
| $C_4$ | $\sigma_{iso}^{orb}$ | 150.9 | 151.0 | 151.4 | 151.3 | 151.4 | 151.3 | 151.4 | 151.6 | 152.2 | 152.3 | 151.3 | 151.4 | 152.2 |
| | $\sigma^{con}$ | −928 | −852 | −969 | −965 | −1009 | −946 | −961 | −971 | −1095 | −1241 | −964 | −1138 | −1228 |
| | $\sigma_{iso}$ | −777 | −701 | −818 | −814 | −858 | −795 | −810 | −819 | −943 | −1089 | −813 | −987 | −1076 |
| $C_5$ | $\sigma_{iso}^{orb}$ | 156.9 | 157.0 | 157.1 | 157.1 | 156.9 | 157.0 | 157.0 | 157.0 | 157.6 | 157.9 | 157.0 | 157.3 | 158.0 |
| | $\sigma^{con}$ | −365 | −337 | −354 | −361 | −394 | −359 | −380 | −384 | −306 | −268 | −380 | −340 | −267 |
| | $\sigma_{iso}$ | −208 | −180 | −197 | −204 | −237 | −202 | −223 | −227 | −148 | −110 | −223 | −183 | −109 |
| $C_6$ | $\sigma_{iso}^{orb}$ | 156.9 | 157.2 | 156.8 | 156.9 | 156.9 | 157.0 | 156.9 | 156.7 | 157.4 | 157.9 | 156.9 | 157.5 | 157.9 |
| | $\sigma^{con}$ | −409 | −439 | −363 | −361 | −373 | −394 | −384 | −381 | −339 | −271 | −383 | −313 | −269 |
| | $\sigma_{iso}$ | −252 | −282 | −206 | −204 | −216 | −237 | −227 | −224 | −182 | −113 | −226 | −156 | −111 |
| $C_7$ | $\sigma_{iso}^{orb}$ | 151.3 | 150.9 | 151.3 | 151.4 | 151.3 | 151.2 | 151.4 | 151.6 | 151.6 | 152.3 | 151.4 | 152.3 | 152.2 |
| | $\sigma^{con}$ | −1185 | −1258 | −978 | −965 | −995 | −1108 | −975 | −978 | −1156 | −1246 | −979 | −1103 | −1245 |
| | $\sigma_{iso}$ | −1034 | −1107 | −827 | −814 | −844 | −957 | −824 | −826 | −1004 | −1094 | −828 | −951 | −1093 |
| $C_8$ | $\sigma_{iso}^{orb}$ | 61.6 | 61.7 | 43.6 | 44.1 | 46.0 | 47.8 | 52.7 | 54.9 | 56.1 | 57.3 | 52.9 | 54.3 | 55.3 |
| | $\sigma^{con}$ | −746 | −694 | −703 | −643 | −754 | −751 | −645 | −750 | −737 | −631 | −713 | −715 | −657 |
| | $\sigma_{iso}$ | −684 | −632 | −659 | −599 | −708 | −703 | −592 | −695 | −681 | −574 | −660 | −661 | −602 |
| $C_9$ | $\sigma_{iso}^{orb}$ | 5.6 | 5.5 | 10.1 | 8.1 | 10.0 | 9.8 | 8.4 | 6.3 | 6.0 | 5.8 | 5.8 | 5.7 | 5.4 |
| | $\sigma^{con}$ | 505 | 474 | −175 | −122 | −170 | −182 | 175 | 274 | 199 | 130 | 240 | 195 | 123 |
| | $\sigma_{iso}$ | 511 | 480 | −165 | −114 | −160 | −172 | 183 | 280 | 205 | 136 | 246 | 201 | 128 |
| $C_{10}$ | $\sigma_{iso}^{orb}$ | 51.4 | 51.3 | 59.3 | 57.4 | 56.3 | 55.0 | 59.0 | 58.1 | 58.0 | 58.0 | 55.9 | 55.9 | 55.6 |
| | $\sigma^{con}$ | −137 | −113 | 252 | 194 | 306 | 404 | −128 | −257 | −176 | −112 | −202 | −170 | −104 |
| | $\sigma_{iso}$ | −86 | −62 | 311 | 251 | 362 | 459 | −69 | −199 | −118 | −54 | −146 | −114 | −48 |

[a] $\sigma_{iso}^{orb}$ was calculated with P86, $\sigma^{con}$ with B3LYP. $\sigma_{iso}$ is the sum of $\sigma_{iso}^{orb}$ (SOS) and $\sigma^{con}$ evaluated at 314 K. [b] 2-OHPhNN was optimized with UB3LYP. [c] 2-OHPhNN was optimized with ROB3LYP.

the solution data. In general, the qualitative and sometimes quantitative picture of the arrangement of hydrogen chemical shifts is realized by our investigation.

The $\sigma_{iso}$ for protons, decomposed into $\sigma_{iso}^{orb}$ and $\sigma^{con}$ contributions, are collected in Table 5. All calculated $\sigma_{iso}^{orb}$ data are positive, therefore orbital shielding of protons has a diamagnetic character; the paramagnetic second-order contribution is small when compared to the corresponding first-order diamagnetic. For example, in the 3-OHPhNN·$2H_2O$ complex, the diamagnetic orbital contributions are 31.1 ppm for $^1H_{para}$, 29.6 ppm for $^1H_{meta}$, and 25.9 ppm for $^1H_{OH}$; the paramagnetic orbital contributions are −7, −5.6, and −3.9 ppm, respectively. All $\sigma^{orb}$ values are distributed in the range of 20−30 ppm, increasing from the hydroxy group proton to the averaged results for the methyl protons. The contact part is smaller in magnitude than $\sigma^{orb}$; the only exception is $\sigma^{con}$ of $^1H_{OH}$ in the ortho-substituted case (for example, 57.5 ppm, calculated at 305 K using the RO-optimized molecular structure, the corresponding $\sigma^{orb}$ is 21.3 ppm). This fact can easily be explained by intramolecular hydrogen-bond formation that assists the spin-density transfer and increases the contact part significantly.

### Hydrogen Bonding Influence on the NMR Data

We already mentioned above that the SOMO is distributed over the two NO fragments of the imidazolyl ring with the main influence on $C_1$ that is located at a node in the SOMO. Despite the limited delocalization of this electron over the phenoxyl substituent, spin polarization is permitted. The intramolecular polarization of the conjugated phenyl ring's system, brought about by an overlap of the SOMO of imidazolyl with the $\pi$ MO of phenyl, leads to the alternation of the electron density in the conjugated chain. In the case of molecules and complexes considered in our work, negative spin density is induced to the carbons at ortho ($C_9$ in the 2-OHPhNN and $C_{10}$ in the 3-OHPhNNs) and para positions ($C_9$ in 4-OHPhNNs and 4-OMePhNNs) of the phenyl ring as well as at the carbons of the imidazolyl ring skeleton. The opposite is found for the methyl group carbons ($C_4$−$C_7$) and $C_8$ of the phenyl ring.

The isotropic hyperfine coupling constant, $A_{iso}$, is determined by electron spin density at the nucleus,[25] and due to the relation between $A_{iso}$ and contact shift observed in the NMR spectra of paramagnetic molecules (see eqs 2 and 6), one−one correspondence between contact shift and spin density exists.[58] Furthermore, contact shift changes going from one NMR active nucleus to another one allow us to map the electron spin-density variation pattern in molecule when all experimental measurements obtained at the same temperature.

To summarize the magnetic behavior for the NNs considered in our investigation, 3-OHPhNN presents predominantly antiferromagnetic interaction (mainly as a result of closeness of SOMOs of radicals in different dimers); 4-OHPhNN has a

**TABLE 4: $^1$H NMR Chemical Shifts ($\delta$, in ppm) for *n*-OH(OMe)PhNNs and Their Complexes with *n* Water Molecules ( $n = 1, 2, 3$)[a]**

| type of compound | $^1H^{ax/eq}$ | $^1H_{meta}$ | $^1H_{para}$ | $^1H_{OH}$ |
|---|---|---|---|---|
| | | Ortho-Substituted Compound | | |
| 2-OHPhNN | −11.9 (−11.5) | −7.3 (−6.9) | 39.4 (38.5) | −48.5 (−46.8) |
| 2-OHPhNN | −11.6 (−11.3) | −5.0 (−4.6) | 35.3 (34.5) | −47.5 (−45.9) |
| exp[b] | −13.2 (−) | −5.0 (−) | 29.9 (29.3) | |
| | | Meta-Substituted Complexes | | |
| 3-OHPhNN | −14.3 (−13.8) | 0.4 (0.5) | 44.0 (43.2) | 4.3 (4.3) |
| 3-OHPhNN·$H_2O$ | −14.0 (−13.6) | −2.3 (−2.0) | 37.8 (36.7) | 8.9 (8.9) |
| 3-OHPhNN·$2H_2O$ | −14.4 (−13.8) | −3.9 (−3.3) | 45.3 (44.2) | 8.3 (8.3) |
| 3-OHPhNN·$3H_2O$ | −13.5 (−13.2) | −11.0 (−10.4) | 46.5 (45.4) | 7.4 (7.4) |
| exp[b] | −14.2 (−) | −5.6 (−) | 35.6 (40.0) | 7.9 (−) |
| | | Para-Substituted Complexes | | |
| 4-OHPhNN | −14.6 (−14.1) | 5.5 (5.5) | | 15.3 (15.0) |
| 4-OHPhNN·$H_2O$ | −14.7 (−14.2) | −15.1 (−13.2) | | 19.6 (19.3) |
| 4-OHPhNN·$2H_2O$ | −12.9 (−12.5) | −3.0 (−2.4) | | 22.0 (21.8) |
| 4-OHPhNN·$3H_2O$ | −10.6 (−10.2) | 2.9 (3.2) | | 18.4 (18.2) |
| exp[b] | −14.7 (−) | 5.1 (−) | | 8.6 (−) |
| | | Methoxy-Substituted Complexes | | |
| 4-OMePhNN | −14.7 (−14.3) | −4.7 (−4.3) | | |
| 4-OMePhNN·$H_2O$ | −13.0 (−12.6) | −4.6 (−4.3) | | |
| 4-OMePhNN·$2H_2O$ | −10.2 (−9.9) | 3.4 (3.5) | | |
| exp[b] | −14.6 (−) | −5.2 (−) | | |

[a] Results were derived using the formula $\delta = \sigma_{iso}^{ref} - \sigma_{iso}^{orb} - \sigma^{con} + \delta^0$. The $^1$H signal, experimentally at $\delta^0 = 2.0$ ppm, in adamantane was used as an external chemical shift reference. UKS/IGLO-III/F32 calculation with the P86 exchange-correlation functional gives $\sigma_{iso}^{ref}$ ($^1$H) = 29.32 ppm for the reference system from ref 33. In calculated results, the first number corresponds to the chemical shift calculated with $\sigma^{con}$ evaluated at 305 K, and the second with $\sigma^{con}$ evaluated at 314 K, respectively. [b] Experimental data of NMR in solution (first number) and MAS NMR (second number) are from ref 29.

**TABLE 5: $^1$H Isotropic Shielding Constants (in ppm) for *n*-OH(OMe)PhNNs and Their Complexes with *n* Water Molecules ( $n = 1, 2, 3$)[a]**

| | $^1H^{ax/eq}$ | | | $^1H_{OH}$ | | | $^1H_{meta}$ | | | $^1H_{para}$ | | |
|---|---|---|---|---|---|---|---|---|---|---|---|---|
| type of compound | $\sigma_{iso}^{orb}$ | $\sigma^{con}$ | $\sigma_{iso}$ | $\sigma_{iso}^{orb}$ | $\sigma^{con}$ | $\sigma_{iso}$ | $\sigma_{iso}^{orb}$ | $\sigma^{con}$ | $\sigma_{iso}$ | $\sigma_{iso}^{orb}$ | $\sigma^{con}$ | $\sigma_{iso}$ |
| | | | | | Ortho-Substituted Compound | | | | | | | |
| 2-OHPhNN | 29.85 | 13.4 (13.0) | 43.25 (42.85) | 21.5 | 58.3 (56.6) | 79.8 (78.1) | 24.4 | 14.2 (13.8) | 38.6 (38.2) | 23.6 | −31.7 (−30.8) | −8.1 (−7.2) |
| 2-OHPhNN | 29.87 | 13.1 (12.8) | 42.97 (42.67) | 21.3 | 57.5 (55.9) | 78.8 (77.2) | 24.4 | 12.1 (11.7) | 36.5 (36.1) | 23.6 | −27.6 (−26.8) | −4.0 (−3.2) |
| | | | | | Meta-Substituted Complexes | | | | | | | |
| 3-OHPhNN | 29.95 | 15.6 (15.2) | 45.55 (45.15) | 27.3 | −0.3 (−0.3) | 27.0 (27.0) | 23.8 | 7.2 (7.0) | 31.0 (30.8) | 24.5 | −37.5 (−36.4) | −13.0 (−11.9) |
| 3-OHPhNN·$H_2O$ | 29.93 | 15.4 (15.0) | 45.33 (44.93) | 22.6 | −0.2 (−0.2) | 22.4 (22.4) | 24.0 | 9.6 (9.3) | 33.6 (33.3) | 24.4 | −30.7 (−29.8) | −6.5 (−5.4) |
| 3-OHPhNN·$2H_2O$ | 29.94 | 15.8 (15.2) | 45.74 (45.14) | 22.0 | 1.0 (1.0) | 23.0 (23.0) | 23.9 | 11.3 (10.7) | 35.2 (34.6) | 24.1 | −38.1 (−37.0) | −14.0 (−12.9) |
| 3-OHPhNN·$3H_2O$ | 29.92 | 14.9 (14.6) | 44.82 (44.52) | 22.0 | 1.9 (1.9) | 23.9 (23.9) | 23.7 | 18.6 (18.0) | 42.3 (41.7) | 24.1 | −39.3 (−38.2) | −15.2 (−14.1) |
| | | | | | Para-Substituted Complexes | | | | | | | |
| 4-OHPhNN | 29.93 | 16.0 (15.5) | 45.93 (45.43) | 26.9 | −10.9 (−10.9) | 16.0 (16.0) | 24.3 | 1.5 (1.5) | 25.8 (25.8) | | | |
| 4-OHPhNN·$H_2O$ | 29.95 | 16.0 (15.5) | 45.95 (45.45) | 22.1 | −10.4 (−10.1) | 11.7 (12.0) | 24.3 | 22.1 (20.2) | 46.4 (44.5) | | | |
| 4-OHPhNN·$2H_2O$ | 29.88 | 14.4 (14.0) | 44.28 (43.88) | 22.0 | −12.8 (−12.5) | 9.2 (9.5) | 24.4 | 9.9 (9.3) | 34.3 (33.7) | | | |
| 4-OHPhNN·$3H_2O$ | 29.75 | 12.2 (11.8) | 41.95 (41.55) | 21.9 | −9.0 (−8.8) | 12.9 (13.1) | 24.3 | 4.1 (3.8) | 28.4 (28.1) | | | |
| | | | | | Methoxy-Substituted Complexes | | | | | | | |
| 4-OMePhNN | 29.95 | 16.1 (15.6) | 46.05 (45.55) | | | | 21.3 | 14.7 (14.3) | 36.0 (35.6) | | | |
| 4-OMePhNN·$H_2O$ | 29.85 | 14.5 (14.0) | 44.35 (43.85) | | | | 24.3 | 11.6 (11.3) | 35.9 (35.6) | | | |
| 4-OMePhNN·$2H_2O$ | 29.73 | 11.8 (11.5) | 41.53 (41.23) | | | | 24.3 | 3.6 (3.5) | 27.9 (27.8) | | | |

[a] $\sigma_{iso}^{orb}$ was calculated with P86. $\sigma^{con}$ evaluated with B3LYP and conforms to 305 K (first number) and at 314 K (second number), respectively. $\sigma_{iso}$ is the sum of $\sigma_{iso}^{orb}$ and $\sigma^{con}$ evaluated at the two temperatures.

ferromagnetic order.[56] 4-SMePhNN, the structure of which is very similar to 4-OMePhNN, is a bulk ferromagnet.[56]

The ability of hydrogen bonds to propagate magnetic interaction is well known. Therefore, the paramagnetic NMR shieldings of $C_4-C_7$, $C_9$, and the $H_{OH}$ closest to the hydrogen-bonding site of the present systems were considered in this section.

The good agreement between experimentally determined and theoretically evaluated chemical shifts in the cases of 3-OHPhNN·$2H_2O$, 4-OHPhNN·$2H_2O$, and 4-OMePhNN·$H_2O$ allow us to justify the use of these structures as the most suitable candidates for a crystal model. Therefore we limit our consideration up to this order of hydrogen bonding. Since the magnetic behavior of each type of complexes are different, one can assume that some difference in changes of $\sigma^{con}$, and therefore in the changes of spin densities on the defined nuclei, can be distinguished.

Assuming that the para and methoxy substitutes are magnetically similar in nature, we expected that changes in $\sigma^{con}$ for both of these final complexes go in the same direction. In fact, the contact shieldings for the axial carbons ($C_4$ and $C_7$) of the imidazolyl ring become more negative compared with their previous structure (4-OHPhNN·$H_2O$ and 4-OMePhNN, respectively). On the other hand, the values of $\sigma^{con}$ for equatorial carbons ($C_5$ and $C_6$) become more positive. The presence of efficient hyperconjugation between the SOMO and the axial bonds assists accumulation of positive spin density on $C_4$ and $C_7$; the opposite is found for $C_5$ and $C_6$. Figure 5 shows the

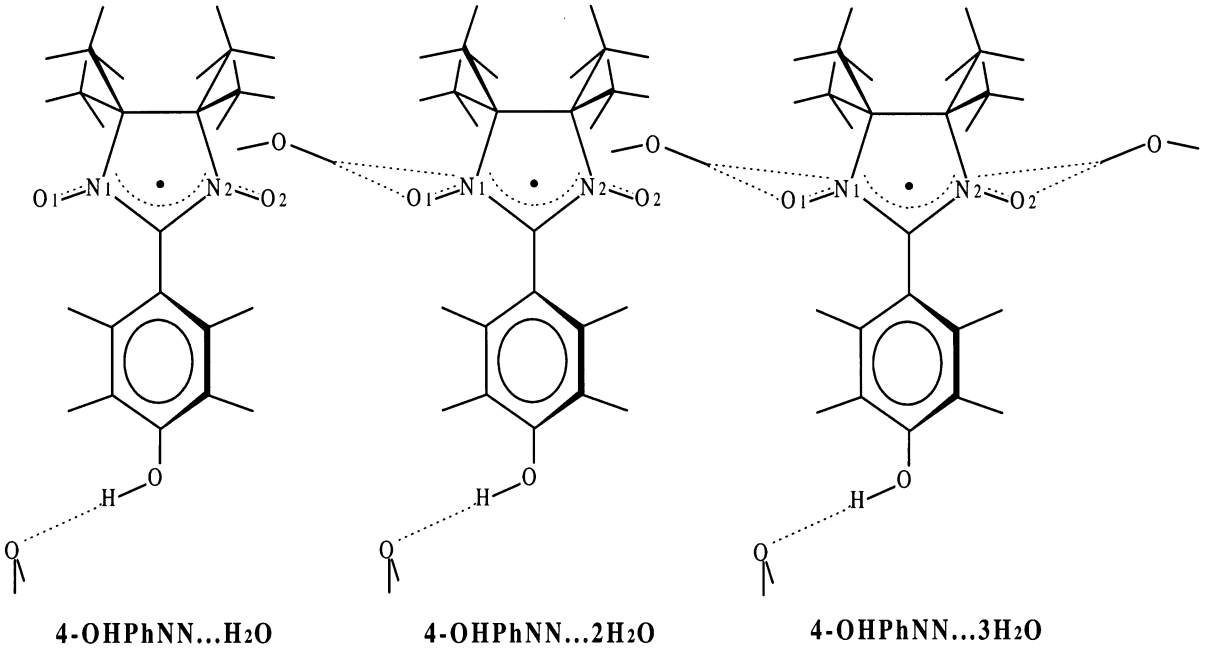


**Figure 3.** *p*-Hydroxyphenyl nitronylnitroxide complexes with *n* water molecules ($n = 1, 2, 3$).

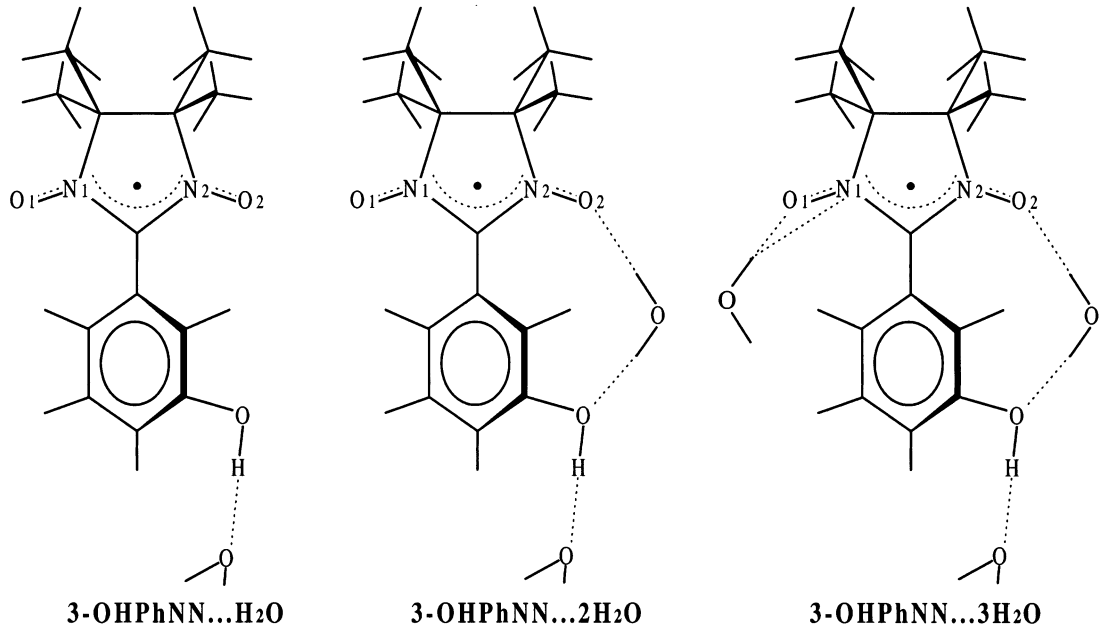


**Figure 4.** *m*-Hydroxyphenyl nitronylnitroxide complexes with *n* water molecules ($n = 1, 2, 3$).

computed spin density for the chosen nuclei as functions of the number of water molecules hydrogen bonded to the parent compounds. The equatorial methyl groups in which $C_5$ and $C_6$ included are important; in the crystal structure, the connection between molecular chains are realized through CH···ON hydrogen bonds. The resulting two-dimensional sheet for the para substitute, for example, is virtually flat.[56]

The corresponding changes in $\sigma^{con}$ of $C_9$ are also identical in these two types of complexes, otherwise we observe here the reduction of negative spin population caused by the changes in the spin density distribution in imidazolyl ring during the process of hydrogen bond of NO···HO type formation. The initial increase of $\sigma^{con}$, observed in the case of 4-OHPhNN·$H_2O$, is due to the fact that the first water molecule is bonded with the phenyl ring OH group of which the hydrogen atom ($H_{OH}$) is the acceptor. Then, such a reduction simultaneously assists the changes in the spin density of $H_{OH}$ (see Figure 6). Because of the presence of the neighboring oxygen that is influenced by $C_9$, $\sigma^{con}$ for $H_{OH}$ becomes more negative (going from one- to two-water complexes), i.e., the positive spin density increases on this proton and makes an interaction with the donor (oxygen in water in model or oxygen in ON in real crystal) stronger.

A similar picture is observed for changes of $\sigma^{con}$ in the meta substitutes, for $C_4$, $C_7$, and $C_9$ (going from one-water to two-water complexes). All of these $\sigma^{con}$ are shifted to the negative. The expected difference between the meta and previously considered complexes arises from the fact that $\sigma^{con}$ for equatorial carbons change in the same manner as for previous nuclei of meta molecules and also become more negative. Therefore, the positive spin density on these nuclei ($C_5$ and $C_6$) increases, that cannot be accidental taking into account the antiferromagnetic nature of meta crystals.

At the same time, $\sigma^{con}$ of $H_{OH}$ in meta complexes constantly increases and in the case of the two-water complex even changes

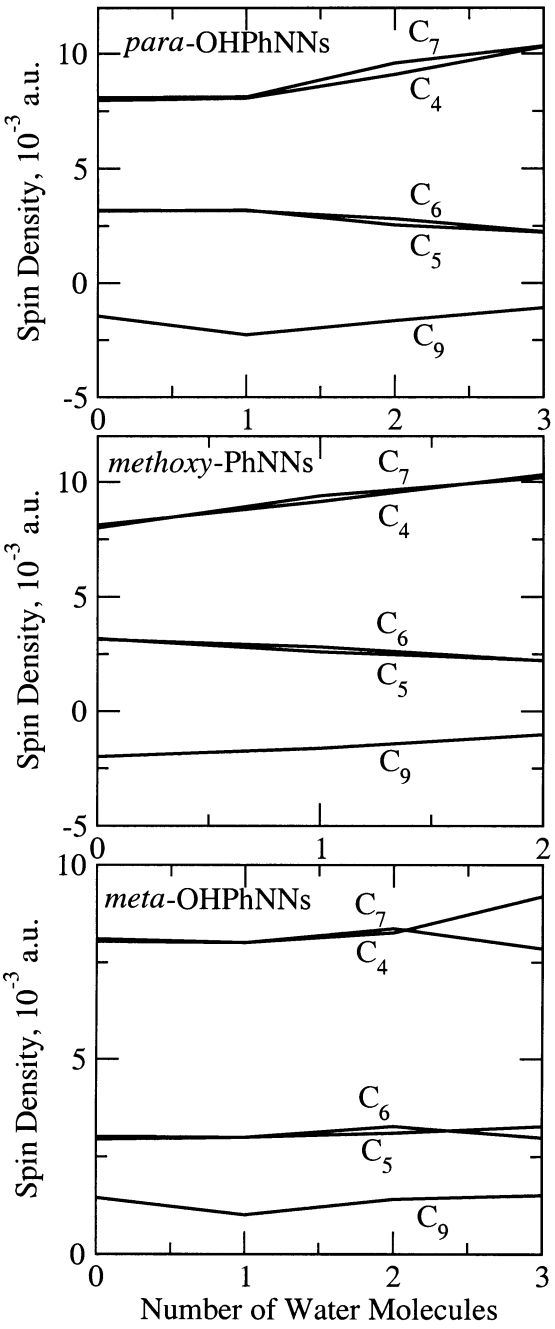


**Figure 5.** The variation of the calculated spin density of carbon nuclei in the *m*- and *p*-hydroxyphenyl and methoxyphenyl nitronylnitroxide complexes, with the number of water molecules hydrogen bonded to the parent compound.

the sign; therefore an initially positively polarized proton obtains a small negative spin density. This fact can indicate an efficient interaction between molecules in a dimer unit. We can suggest that because of this strong interaction, the corresponding changes in $\sigma^{con}$ of $C_5$ and $C_6$ are also observed.

## Conclusions

A density functional method has been applied for calculating nuclear-shielding tensors in open-shell, paramagnetic, NN molecules. The used nonrelativistic approach is consistent up to $O(\alpha^2)$ in the fine-structure constant $\alpha$. The total nuclear shielding contains an orbital contribution in accordance with Ramsey's theory for shielding in closed-shell systems and temperature-dependent, fully isotropic Fermi contact as well as fully anisotropic dipolar contributions.

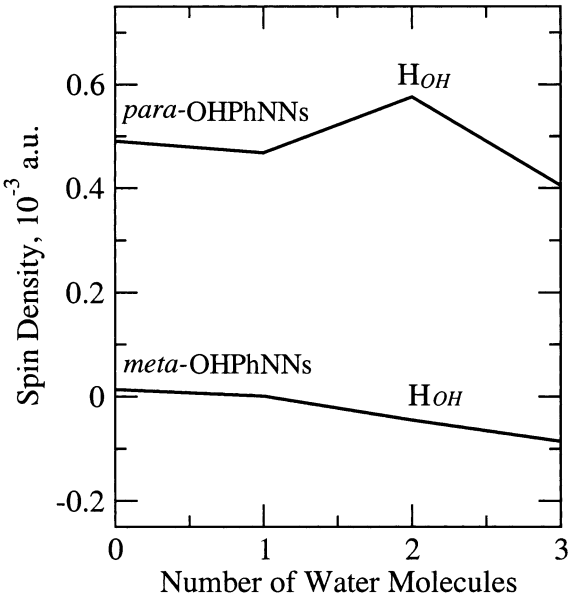


**Figure 6.** The variation of the calculated spin density of $^1H_{OH}$ nuclei in the *m*- and *p*-hydroxyphenyl nitronylnitroxide complexes, with the number of water molecules hydrogen bonded to the parent compound.

DFT calculations were carried out for *o*-, *m*-, and *p*-hydroxyphenyl NN, as well as for methoxyphenyl NN and their complexes with hydrogen-bonded water molecules. The direction of hydrogen bonding corresponds to the real crystal environment. The good quality of results for geometry optimization in the RO procedure justifies the use of these geometries instead of those resulting from the unrestricted approach.

A combined method was applied for calculations of the nuclear shieldings; the orbital terms were calculated using the generalized gradient approximation and the contact parts using the hybrid B3LYP functional in unrestricted DFT. This gives qualitative agreement with available experimental data and reproduces well the signs and trends in the NMR chemical shifts. Such a level of accuracy has been achieved, first of all, through the inclusion of the essential part of matrix effects by the hydrogen bonds. On the other hand, significant errors in some shieldings are introduced by the basis set incompleteness and DFT errors, as well as matrix effects (other than described by the strong hydrogen bonds), and motional averaging.

The orbital contributions, $\sigma_{iso}^{orb}$, to the nuclear-shielding constants in the considered NN complexes are nonnegligible in comparison with the contact term. The $\sigma_{iso}^{orb}$ values are positive for all carbons and hydrogens, indicating that the first-order $\langle 0|H^{DS}_{K,B_0}|0\rangle$ contribution[33] to $\sigma_{iso}^{orb}$ is predominant. The second-order paramagnetic contribution to $\sigma_{iso}^{orb}$ is also important, and its changes are reflected in the $\sigma_{iso}^{orb}$ values for the atoms of the imidazolyl ring, on which the delocalized unpaired electron mainly acts, and for the carbon atom of the phenyl ring connected with the OH group, on which the neighboring oxygen acts.

The contact shieldings, $\sigma^{con}$, that are the main contributions to the chemical shifts, are strongly dependent on the number of hydrogen bonds. It is found that the tendency of $\sigma^{con}$ to change directly corresponds to the spin delocalization pattern in these molecules. Three different effects influence the direction of the spin density transfer, first the bonding of a water molecule with the OH group in the phenyl ring, second two water molecules bonded with the iminoxyl groups in the imidazolyl ring, and last a polarization, induced by the mutual influence of the rings. All these effects are important and contribute to the changes of

$\sigma^{con}$. We have found that for magnetically similar complexes the changes to $\delta^{con}$ or the corresponding changes in the spin densities are largely parallel.

**Acknowledgment.** We warmly thank Professor Frank H. Köhler (Anorganisch-chemisches Institut, Technische Universität München) for useful discussions and for providing the additional experimental MAS NMR information not included in ref 29. J.V. is an Academy Fellow of the Academy of Finland and on leave from the NMR Research Group, University of Oulu, Finland. He is further supported by the Magnus Ehrnrooth Fund as well as by the Vilho, Yrjö, and Kalle Väisälä Foundation. Z.R. acknowledges the support from the EU network "Molecular Properties and Molecular Materials" (MOLPROP, Contract HPRN-CN-2000-0013). O.V. acknowledges support from the Swedish Research Council (VR) and the Magnus Bergvall Foundation. The computational resources were partially provided by the Center for Scientific Computing, Espoo, Finland.

## References and Notes

(1) Yakhmi, J. V. *Physica B* **2002**, *321*, 204−212.

(2) Osiecki, J. H.; Ullman, E. F. *J. Am. Chem. Soc.* **1968**, *90*, 1078−1079.

(3) Swartz, H. M. *Pure. Appl. Chem.* **1990**, *62*, 235−239.

(4) Sueki, M.; Eaton, G. R.; Eaton, S. S. *Pure. Appl. Chem.* **1990**, *62*, 229−233.

(5) Aurich, H. G. In *Nitrones, Nitronates and Nitroxides*; Patai, S., Rappoport, Z., Eds.; Wiley: Chichester, 1989; pp 313−369.

(6) Saint-Paul, M.; Veyret, C. *Phys. Lett. A* **1973**, *45*, 362−364.

(7) Kinoshita, M.; Turek, P.; Tamura, M.; Nozawa, K.; Shiomi, D.; Nakazawa, Y.; Ishikawa, M.; Takahashi, M.; Agawa, K.; Inabe, T.; Maruyama, Y. *Chem. Lett.* **1991**, 1225−1228.

(8) Tamura, M.; Nakazawa, Y.; Shiomi, D.; Nozawa, K.; Hosokoshi, Y.; Ishikawa, M.; Takahashi, M.; Kinoshita, M. *Chem. Phys. Lett.* **1991**, *186*, 401−404.

(9) Nakatsuji, S.; Anzai, H. *J. Mater. Chem.* **1997**, *7*, 2161−2174.

(10) Gatteshi, D.; Carretta, P.; Lascialfari, A. *Physica B* **2000**, *289−290*, 94−105.

(11) Deumal, M.; Cirujeda, J.; Veciana, J.; Novoa, J. J. *Adv. Mater.* **1998**, *10*, 1461−1466.

(12) Ballester, G.; Coronado, E.; Galán-Mascarós, J. R.; Giménez-Saiz, C.; Nuez, A.; Romero, F. M. *Polyhedron* **2001**, *20*, 1659−1662.

(13) Cirujeda, J.; Mas, M.; Molins, E.; Lanfranc de Panthou, F.; Laugier, J.; Park, J. G.; Paulsen, C.; Rey, P.; Rovira, C.; Veciana, J. *J. Chem. Soc., Chem. Commun.* **1995**, 709−710.

(14) Chiarelli, R.; Novak, M. A.; Rassat, A.; Tholence, J. L. *Nature (London)* **1993**, *363*, 147−149.

(15) Deumal, M.; Cirujeda, J.; Veciana, J.; Kinoshita, M.; Hosokoshi, Y.; Novoa, J. J. *Chem. Phys. Lett.* **1997**, *265*, 190−199.

(16) Kinoshita, M. In *Handbook of Organic Conductive Molecules and Polymers*; Halwa, H. S., Ed.; Wiley: New York, 1997; Vol. 1, pp 781−800.

(17) Cirujeda, J.; Vidal-Gancedo, J.; Jürgens, O.; Mota, F.; Novoa, J. J.; Rovira, C.; Veciana, J. *J. Am. Chem. Soc.* **2000**, *122*, 11393−11405.

(18) Davis, M. S.; Morokuma, K.; Kreilick, R. W. *J. Am. Chem. Soc.* **1972**, *94*, 5588−5592.

(19) Jürgens, O.; Cirujeda, J.; Mas, M.; Mata, I.; Cabrero, A.; Vidal-Gancedo, J.; Rovira, C.; Molins, E.; Veciana, J. *J. Mater. Chem.* **1997**, *7*, 1723−1730.

(20) Minguet, M.; Amabilino, D. B.; Mata, I.; Molins, E.; Veciana, J. *Synth. Met.* **1999**, *103*, 2253−2256.

(21) Neely, J. W.; Hatch, G. F.; Kreilick, R. W. *J. Am. Chem. Soc.* **1974**, *96*, 652−656.

(22) Stroh, C.; Romero, F. M.; Kyritsakas, N.; Catala, L.; Turek, Ph.; Ziessel, R. *J. Mater. Chem.* **1999**, *9*, 875−882.

(23) Deumal, M.; Lafuente, P.; Mota, F.; Novoa, J. J. *Synth. Met.* **2001**, *122*, 477−483.

(24) Deumal, M.; Novoa, J. J. *THEOCHEM* **2000**, *506*, 287−296.

(25) Bertini, I.; Luchinat, C.; Parigi, G. *Solution NMR of Paramagnetic Molecules*; Elsevier: Amsterdam, 2001.

(26) Horrocks, W. DeW., Jr. In *NMR of Paramagnetic Molecules. Principles and Applications*; La Mar, G. N., Horrocks, W. DeW., Jr., Holm, R. H., Eds.; Academic Press: New York, London, 1973; pp 128−175.

(27) Stejskal, E. O.; Memory, J. D. *High-Resolution NMR in the Solid State. Fundamentals of CP/MAS*; Oxford University Press: New York, 1994.

(28) Groombridge, C. J.; Perkins, M. J. *J. Chem. Soc., Chem. Commun.* **1991**, 1164.

(29) Heise, H.; Köhler, F. H.; Mota, F.; Novoa, J. J.; Veciana, J. *J. Am. Chem. Soc.* **1999**, *121*, 9659−9667.

(30) Lahti, P. M. *Magnetic Properties of Organic Materials*; Marcel Dekker: New York, 1999; pp 540−545.

(31) Romero, F. M.; Ziessel, R.; Bonnet, M.; Pontillon, Y.; Ressouche, E.; Schweizer, J.; Delley, B.; Grand, A.; Paulsen, C. *J. Am. Chem. Soc.* **2000**, *122*, 1298−1309.

(32) Ramsey, N. F. *Phys. Rev.* **1950**, *78*, 699−703.

(33) Rinkevicius, Z.; Vaara, J.; Telyatnyk, L.; Vahtras, O. *J. Chem. Phys.* **2003**, *118*, 2550−2561.

(34) Frisch, M. J.; Trucks, G. W.; Schlegel, H. B.; Scuseria, G. E.; Robb, M. A.; Cheeseman, J. R.; Zakrzewski, V. G.; Montgomery, J. A., Jr.; Stratmann, R. E.; Burant, J. C.; Dapprich, S.; Millam, J. M.; Daniels, A. D.; Kudin, K. N.; Strain, M. C.; Farkas, O.; Tomasi, J.; Barone, V.; Cossi, M.; Cammi, R.; Mennucci, B.; Pomelli, C.; Adamo, C.; Clifford, S.; Ochterski, J.; Petersson, G. A.; Ayala, P. Y.; Cui, Q.; Morokuma, K.; Malick, D. K.; Rabuck, A. D.; Raghavachari, K.; Foresman, J. B.; Cioslowski, J.; Ortiz, J. V.; Stefanov, B. B.; Liu, G.; Liashenko, A.; Piskorz, P.; Komaromi, I.; Gomperts, R.; Martin, R. L.; Fox, D. J.; Keith, T.; Al-Laham, M. A.; Peng, C. Y.; Nanayakkara, A.; Gonzalez, C.; Challacombe, M.; Gill, P. M. W.; Johnson, B. G.; Chen, W.; Wong, M. W.; Andres, J. L.; Head-Gordon, M.; Replogle, E. S.; Pople, J. A. *Gaussian 98*, revision A.7; Gaussian, Inc.: Pittsburgh, PA, 1998.

(35) (a) Becke, A. D. *J. Chem. Phys.* **1993**, *98*, 5648−5652. (b) Stephens, P. J.; Devlin, F. J.; Chabalowski, C. F.; Frisch, M. J. *J. Phys. Chem.* **1994**, *98*, 11623−11627.

(36) Adamo, C.; di Matteo, A.; Rey, P.; Barone, V. *J. Phys. Chem. A* **1999**, *103*, 3481−3488.

(37) (a) The deMon Kohn−Sham program: Salahub, D. R.; Fournier, R.; Mlynarski, P.; Papai, I.; St-Amant, A.; Ushio, J. *Density Functional Methods in Chemistry*; Labanowski, J., Andzelm, J., Eds.; Springer: New York, 1991. (b) St-Amant, A.; Salahub, D. R. *Chem. Phys. Lett.* **1990**, *169*, 387−392.

(38) (a) The magnetic property packages for deMon: Malkin, V. G.; Malkina, O. L.; Eriksson, L. A.; Salahub, D. R. *Modern Density Functional Theory: A Tool for Chemistry; Theoretical and Computational Chemistry*; Seminario, J. M., Politzer, P., Eds.; Elsevier: Amsterdam, 1995; Vol. 2. (b) For the latest version, see: Vaara, J.; Malkina, O. L.; Stoll, H.; Malkin, V. G.; Kaupp, M. *J. Chem. Phys.* **2001**, *114*, 61−71 and ref 39.

(39) Malkina, O. L.; Vaara, J.; Schimmelpfennig, B.; Munzarová, M.; Malkin, V. G.; Kaupp, M. *J. Am. Chem. Soc.* **2000**, *122*, 9206−9218.

(40) Huzinaga, S. *Approximate Atomic Functions*; University of Alberta: Edmonton, 1971.

(41) Kutzelnigg, W.; Fleischer, U.; Schindler, M. In *NMR Basic Principles and Progress*; Diehl, P., Fluck, E., Günther, H., Kosfeld, R., Eds.; Springer: Heidelberg, 1990; Vol. 23, p 165.

(42) Perdew, J. P.; Wang, Y. *Phys. Rev. B* **1986**, *33*, 8800−8802.

(43) Perdew, J. P. *Phys. Rev. B* **1986**, *33*, 8822−8824.

(44) Pipek, J.; Mezey, P. G. *J. Chem. Phys.* **1989**, *90*, 4916−4926.

(45) Kaupp, M.; Malkina, O. L.; Malkin, V. G. *J. Chem. Phys.* **1997**, *106*, 9201−9212.

(46) Malkin, V. G.; Malkina, O. L.; Casida, M. E.; Salahub, D. R. *J. Am. Chem. Soc.* **1994**, *116*, 5898−5908.

(47) Vignale, G.; Rasolt, M.; Geldart, D. J. W. *Adv. Quantum Chem.* **1990**, *21*, 235−253.

(48) Zheludev, A.; Barone, V.; Bonnet, M.; Delley, B.; Grand, A.; Ressouche, E.; Rey, P.; Subra, R.; Schweizer, J. *J. Am. Chem. Soc.* **1994**, *116*, 2019−2027.

(49) Cirujeda, J.; Rovira, C.; Veciana, J. *Synth. Met.* **1995**, *71*, 1799−1800.

(50) Cirujeda, J.; Hernández-Gasió, E.; Rovira, C.; Stanger, J.-L.; Turek, Ph; Veciana, J. *J. Mater. Chem.* **1995**, *5*, 243−252.

(51) Minguet, M.; Amabilino, D. B.; Wurst, K.; Veciana, J. *J. Solid State Chem.* **2001**, *159*, 440−450.

(52) Yamada, S.; Nakano, M.; Yamaguchi, K. *Chem. Phys. Lett.* **1997**, *276*, 375−380.

(53) Matsushita, M.; Izuoka, A.; Sugawara, T.; Kobayashi, T.; Wada, N.; Takeda, N.; Ishikawa, M. *J. Am. Chem. Soc.* **1997**, *119*, 4369−4379.

(54) Tamura, M.; Shiomi, D.; Hosokoshi, Y.; Iwasawa, N.; Nozawa, K.; Kinoshita, M.; Sawa, H.; Kato, R. *Mol. Cryst. Liq. Cryst.* **1993**, *232*, 45−52.

(55) Awaga, K.; Inabe, T.; Yokoyama, T.; Maruyama, Y. *Mol. Cryst. Liq. Cryst.* **1993**, *232*, 79−88.

(56) Miller, J. S.; Drillon, M. *Magnetism: Molecules to Materials II*; Wiley-VCH: Weinheim, 2001; pp 1−50.

(57) D'Anna, J.; Wharton, J. H. *J. Chem. Phys.* **1970**, *53*, 4047−4052.

(58) The gyromagnetic ratios of both $^{1}H$ and $^{13}C$ are positive. Hence, $A_{iso}$ has the same sign as the spin density at the nucleus, $\sigma^{con}$ is proportional to $-A_{iso}$ (eq 2), and $\delta^{con} = -\sigma^{con}$ again shares the sign with the spin density.